Int. Journ. of Peening Science and Technology, Vol. 1, pp. 119–136
Reprints available directly from the publisher
Photocopying permitted by license only.

© 2018 OCP Materials Science and Engineering
Published by license under the OCP Science imprint,
Old City Publishing, Inc.

Improving the Surface Properties of Ti6Al4V with Laser Shock Processing

CESAR A. REYNOSO-GARCIA[1*], G. GOMEZ-ROSAS[2], O. BLANCO[2], C. RUBIO-GONZALEZ[3], ARTURO CHAVEZ CHAVEZ[2], E. CASTAÑEDA[1] AND J. L. OCANA[4]

[1]*Doctorate in Materials Science, CUCEI, University of Guadalajara, Jose Guadalupe Zuno # 48, Los Belenes, Zapopan, Jalisco, Mexico*
[2]*Department of Physics, CUCEI, University of Guadalajara, Blvd. Marcelino Garcia Barragan #1421, 44430, Guadalajara, Jalisco, México*
[3]*Centre for Engineering and Industrial Development, Av. Playa Pie de la Cuesta No. 702, Desarrollo San Pablo, Queretaro, 76130, Mexico*
[4]*UPM Laser Centre, Polytechnic University of Madrid, Ctra. de Valencia, Km. 7,300. 28031 Madrid, Spain*

Laser shock processing (LSP) is a technique that induces residual compressive stresses in metallic objects through the plastic deformation caused by the propagation of shock waves generated by laser pulses. The alloy Ti6Al4V is utilized in various industries such as the aerospace, automotive, and medical industries. In this study, LSP was performed using a high-power, low-cost, Q-switched Nd:YAG pulsed laser that emits at two wavelengths, 1064 and 532 nm, with pulse times of 6 and 5 ns, respectively. Power densities of 8.4 and 7.5 GW/cm^2 were tested. The material had no protective layer on the surface but was covered with a thin film of water (LSPwC). At both power densities, LSP produced great depth and magnitude residual compressive stresses (a result not previously reported), a reduction in the friction coefficient, and an increase in the hardness were found. The results obtained with both wavelengths were satisfactory and improved the surface properties of Ti6Al4V.

Keywords: *LSP, coefficient of friction, Ti6Al4V, residual stress, hardness, Nd:YAG laser*

1 INTRODUCTION

The alloy Ti6Al4V has low density, high fatigue strength, and excellent corrosion resistance, and this combination of mechanical and physical

*Corresponding author's e-mail: carg23@msn.com

properties makes it desirable in the aerospace industry, where it is used for engine components such as compressor blades [1]. In addition, Ti6Al4V is used in medical prosthetics replacing hip, knee, shoulder, and wrist joints and in dental posts due to its biocompatibility with the human body [2, 3]. However, it is widespread use as a joint component is limited by its low wear resistance both adhesive and abrasive which causes the breakage of the passive layers when the metal enters friction and causes an acceleration in the corrosion and the produced residues are released into the organism [4].

Laser shock processing (LSP), also known as laser shock peening, is a technique that can alter certain mechanical properties of materials by creating a residual stress field to a depth of 1 to 2 mm [5]. The depth of the stress field is greater than that obtained with the abrasive blasting technique [6]. LSP uses high-power laser pulses directed onto the surface of the material. The power density of the laser pulses must be sufficiently high (1 to 10 GW/cm^2) to generate shock waves in the material [7]. These shock waves, upon propagating within the material, lead to plastic deformation that causes structural changes and increases the dislocation density, thereby improving the mechanical properties of the treated material [8]. Previous studies have compared LSP to other surface treatment processes, such as shot peening [9, 10], laser shock forming [11], and deep rolling [12], to determine the benefits of using LSP to treat metal components.

LSP is unique in that a number of treatment parameters and conditions can be varied. The variables include the laser wavelength [13, 14], pulse width [13, 15], power density [16, 17], and energy [3, 18]. An additional option is to apply a protective layer to the material surface to avoid thermal effects due to the plasma generated by LSP [16]. LSP without the protective layer is known as laser peening without coating (LPwC) [19, 20]. LSP also offers options with regard to confinement. One option is water immersion, in which the material is completely submerged in water and is usually irradiated with a wavelength of 532 nm [14]. Another option is water jet confinement, wherein the material is covered by a thin layer of water a few millimetres deep and either the 532 or 1064 nm wavelength can be used with minimal power losses [19].

Several authors in recent years have reported positive results with LSP using a high-power, low-cost Nd:YAG pulsed laser with both water immersion (532 nm) [13] and waterjet confinement (532 nm and 1064 nm) [22].

The LSP technique has shown favourable results in materials such as steel [23], aluminium [24], and titanium [25]. LSP has been applied to the alloy Ti6Al4V in various studies, which have reported that LSP leads to a field of surface deformation and induces residual compressive stresses [26]. Other studies have reported that LSP of Ti6Al4V improves the fretting fatigue [27], increases the micro-hardness [28], and increases the surface roughness [15].

The main objective of this study was to evaluate the effect of LSP on the micro-hardness, surface roughness, microstructure, friction coefficient, and wear of Ti6Al4V without an applied protective layer using a low-cost laser at two different wavelengths with approximately the same power density.

2 EXPERIMENTAL PROCEDURE

2.1 Material Background

A plate of Ti6Al4V manufactured to the ASTM B265 standard was obtained. Square specimens with dimensions of 50 mm × 50 mm × 7 mm were machined and ground with 80 and 100 grit/cm^2 size SiC abrasive paper to eliminate the residual stresses resulting from the manufacturing process.

2.2 Laser Peening

Then, the specimens were irradiated with a Quantel Brilliant B high-energy Nd:YAG pulsed laser with pulses at the fundamental wavelength of 1064 nm for 6 ns. A second optical harmonic coupled to the fundamental wavelength was used to produce pulses at a wavelength of 532 nm for 5 ns. An optical system consisting of mirrors and positive lenses (with a focal length of 1000 mm) was used to direct the laser beam with a diameter of 1.5 mm at 1064 nm and 1.3 mm at 532 nm. The maximum power density was 8.4 GW/cm^2 at 1064 nm and 7.5 GW/cm^2 at 532 nm. A programmable, motorised XY positioning system controlled the location of the beam on the specimen. The LSP treatment was conducted in a square area of 20 mm ´ 20 mm. A pulse density of 2500 pulses/cm^2 was used for both wavelengths, and the overlapping rate was set to achieve the desired distribution of laser pulses on the treated surface [29]. The setup for LSP without a surface coating is shown in Figure 1; the values of additional treatment parameters for both wavelengths are shown in Table 1.

2.3 Blind hole test for Residual Stress

The hole-drilling strain gage method was used to determine the residual stress field induced by LSP in the Ti6Al4V. A CEA-120-06-062UL strain gauge and an RS-200 milling guide with reaming (both items produced by the Vishay Precision Group, Inc.) were used in the tests. The residual compressive stresses were measured according to the ASTM E837-01 standard [30].

2.4 Friction and wear tests

Dry (unlubricated) sliding tests were performed with a Microtest S.A. MT 30 pin-on-disk tribometer. The test parameters are shown in Table 2. The wear tests were repeated four times for each LSP treatment condition and on the untreated material. The software provided with the tribometer (MT4002) was

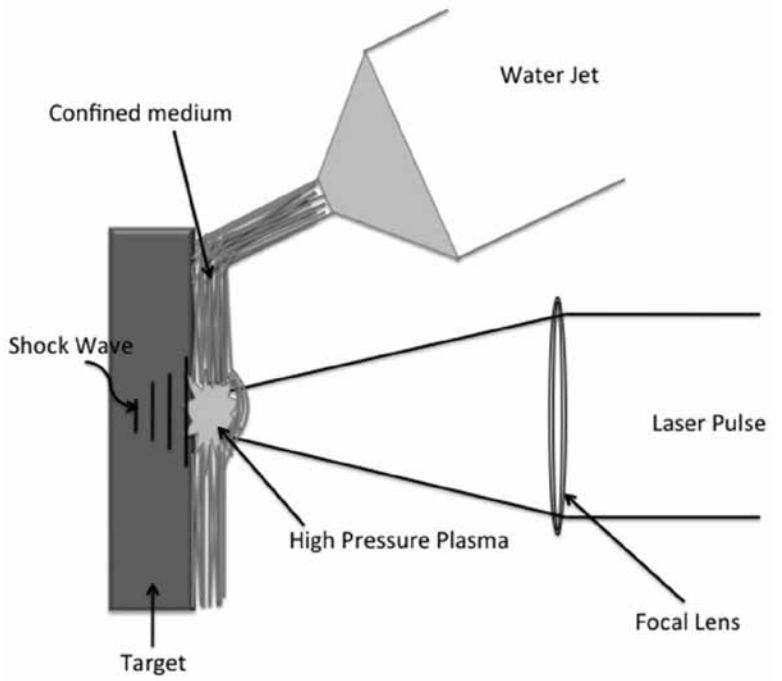

FIGURE 1
Laser shock processing without coating set up.

TABLE 1
LSP treatment parameters.

Wavelength	**1064nm**	**532nm**
Confining mode	Water-Jet	
Ablative coating	No	
Laser	Nd:YAG	
Pulse density	2500 pulses/cm^2	
Spot diameter	1.5 mm	1.3 mm
Pulse duration	6 ns	5 ns
Powerdensity	8.4 GW/cm^2	7.5 GW/cm^2
Energy	0.9 J	0.5 J
Frequency	10 Hz	

used to process the test data, and the coefficient of friction was calculated according to the ASTM G99-04 standard [31].

The friction tests used to obtain the dry slip curves exhibit four stages. The first stage (I) consists of the coupling of the tribological pair (the pin and the disk). In

TABLE 2
Pin-on-disk test parameters.

Speed	**0.0471**	**m/s**
Sliding distance	500	m
Track Radio	1.5	mm
Pin	Steel	AISI 52100
Pin diameter	3	mm
Revolutions	53052	rev
Time	177	min
Load	30	N

the second stage (II), the friction force stabilises. In the third stage (III), a sharp increase in friction occurs, usually catastrophically. In the fourth and final stage (IV), the tribological pair stabilises again and fluctuations occur because of the particles that are released as the result of wear in the tribological pair [32, 33].

2.5 Metallographic analysis

A metallographic analysis was performed according to the ASTM E3-11 standard [34] on cross sections of the treated specimens. The specimens were ground on a Buehler Phoenix® Betagrinding-polishing machine with 240, 400, 800, and 1200 grit/cm^2 size SiC abrasive paper, then polished using 9, 3, and 1 μm diamond suspensions to remove surface scratches. Finally, a mirror finish was obtained by polishing with colloidal silica with a diameter of 0.01 μm. The chemical solution for developing the metallographic samples was a mixture of 190 ml of water, 2 ml of hydrochloric acid, 2 ml of nitric acid, and 2 ml of hydrofluoric acid. The samples were submerged for 30 seconds in the solution. The material phases were examined with scanning electron microscopy (SEM) using a Tescan MIRA3 microscope.

2.6 Phase characterisation

The material phases were determined using a Phillips Expert X-ray diffractometer with a Cu anode (λ= 1.54056). The X-ray diffraction pattern was calculated for each peak over a range of angles from 33.01 to 72.99 degrees.

2.7 Micro-hardness tests

Eight indentations were made 85 microns from each other from the surface of the material to a depth of 1000 microns in the cross-section of the LSP-treated specimens. A Vickers indenter was used to apply a load of 200 g for 20 seconds as prescribed in the ASTM E384 standard. Micro-indentation hardness measurements were performed on the cross-sections of the specimens treated with LSP (from the material surface to a depth of 1 mm). A Vickers indenter was used to apply a load of 200 g for 20 s, as prescribed in the ASTM E384 standard [35].

2.8 Surface roughness

The surface roughness was measured using a Leica confocal scanning laser microscope prior to and subsequent to LSP. The microscope has a scan range of 17 mm in the two horizontal axes (X and Y) and a vertical resolution (Z) of up to 0.01 nm. The measurements were taken over the entire LSP-treated area.

3 RESULTS

3.1 Residual stresses

Figure 2 shows in detail the profiles of the residual stress in the untreated specimen and that treated with LSP with a wavelength of 532 nm and a power density of 7.5 GW/cm^2. The treated specimen had a maximum induced compressive stress of 500 MPa at a depth of 280 μm. The residual stresses at the same depth in the untreated specimen were 280 MPa. Figure 3 shows the profiles of the residual stresses for the untreated specimen and that treated with LSP with a wavelength of 1064 nm and a power density of 8.4 GW/cm^2. The maximum compressive stress was 750 MPa at 325 μm in the treated specimen. The residual compressive stress was 280 MPa in the untreated specimen at the

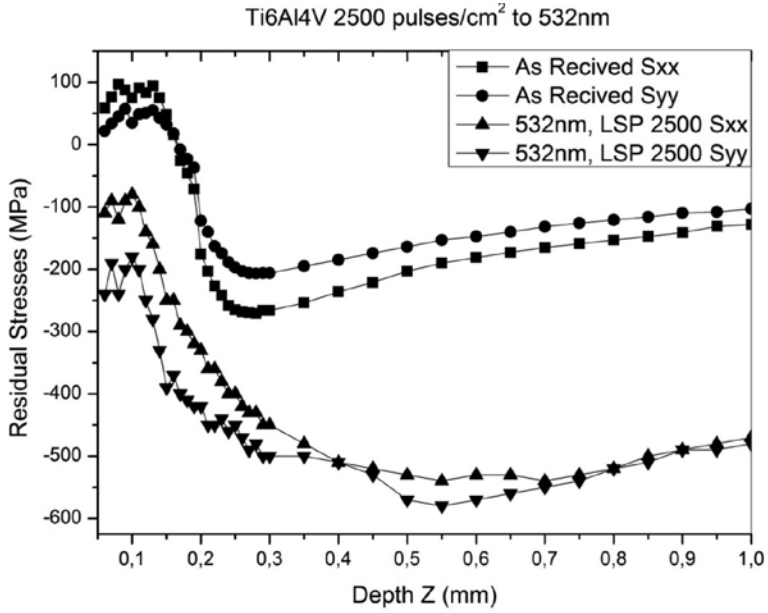

FIGURE 2
In depth residual stresses profile of untreated and processed sample with 532nm. Stress component s_{xx} is parallel while s_{yy} is perpendicular, both to swept direction that will be used during the treatment LSP.

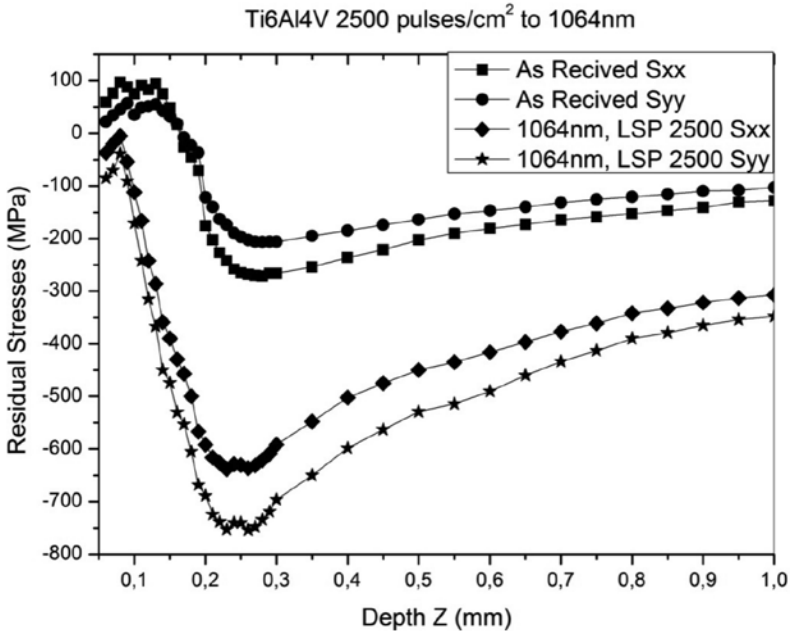

FIGURE 3
In depth residual stresses profile of untreated and processed sample with 1064nm. Stress component s_{xx} is parallel while s_{yy} is perpendicular, both to swept direction that will be used during the treatment LSP.

same depth. The measurements reveal that the residual compressive stresses induced in the Ti6Al4V by LSP with either wavelength were higher in magnitude and extended deeper into the material compared with the untreated specimen. In addition, these values were greater than those previously reported [25].

3.2 Friction

The results of the wear tests on the dry(unlubricated) samples treated with LSP at a power density of 8.4 GW/cm^2 are shown in Figure 4(a). The adjustment stage (I) occurred between 0 and 8 metres, followed by a period of stability in the frictional force (stage II) from 8 to 14 metres. In stage III, a transition can be observed in the untreated specimens. The frictional force on the specimens treated with LSP was stable from 14 to 52 metres. In stage IV, the untreated specimens exhibited frequent transitions and the treated specimens had shorter transitions. The frictional force in the treated samples stabilised again at 77 metres, at which point the abrupt transitions began to occur until the end of the test. The treated specimens had a stable frictional force over a longer distance. In Figure 4(b), the results for the specimens treated with LSP at a power density of 7.5 GW/cm^2 are shown. The lengths of the adjustment stage (I) and the stability period (II) were equal to those observed

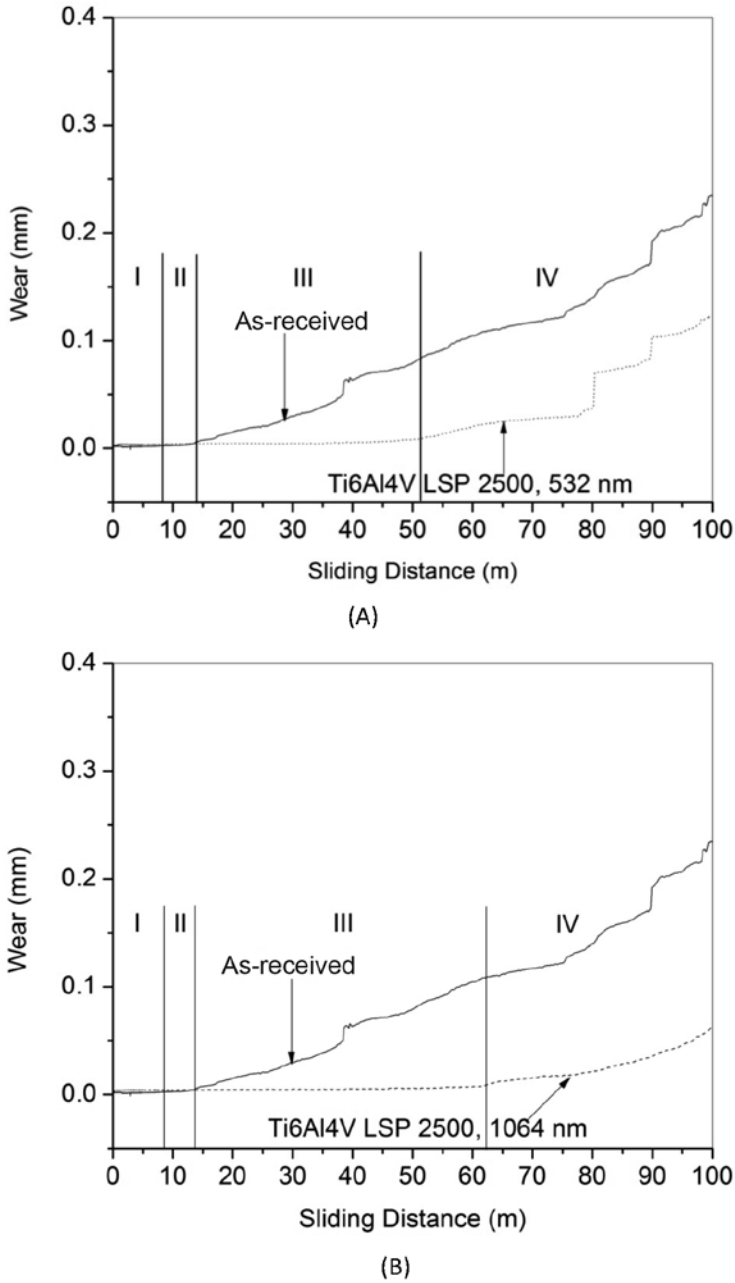

FIGURE 4
Friction force stabilization. Figure 5(a) sample treated with 532nm and figure (b), 1064 nm wavelength.

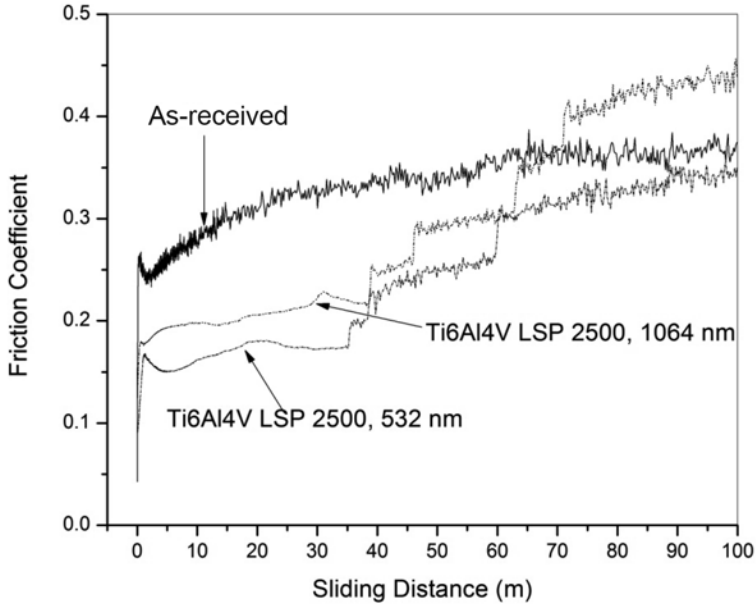

FIGURE 5
Stabilized friction coefficient. Samples without LSP and treated with LSP at 532nm and 1064nm wavelength.

in the specimens treated with a power density of 8.4 GW/cm^2. Stage III in the untreated specimens was characterised by the appearance of the transitions, whereas the frictional force was stable in the treated specimens. During this period (from 14 to 63 metres), small transitions were observed before 63 metres. Beyond this point (in stage IV), transitions occurred in the treated specimens, but no abrupt transitions and instability in the frictional force were observed at 100 metres. The friction test results for the two power densities used showed that the stage of stability of the frictional force was longer in the treated specimens than in the untreated specimens.

3.2.1 Friction Coefficient

Figure 5 shows the results of the friction coefficient of Ti6Al4V. The friction coefficient presented an improvement in the two wavelengths. However, the biggest improvement is in the wavelength of 532nm (0.16). The reduction of the friction coefficient presented could be due to the increase of the hardness and the residual stresses observed after the LSP treatment compared to the material as recived.

On the other hand, there is a difference in wavelengths in the reduction of the friction coefficient. This difference could have two explanations: first, the relationship with the depth of hardness, at a wavelength of 532 nm, a higher hardness (Hv) is obtained up to about 225 microns than at the wavelength of

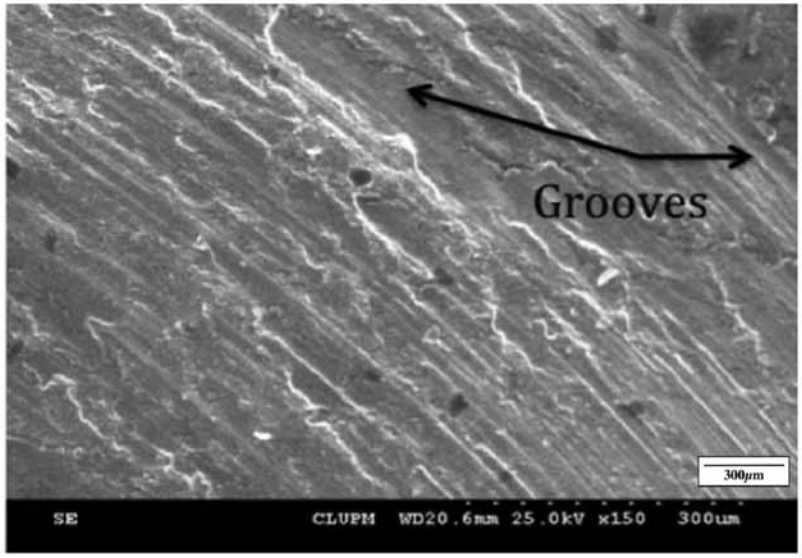

FIGURE 6
Wear systems in material without LSP treatment.

1064 nm (Hv). Secondly, the depth of the residual stresses can be observed that at the wavelength of 532nm reaches its greatest magnitude at a depth of 550μm. However the wavelength of 1064nm has a maximum magnitude at 250 microns in depth, regardless of the magnitude of the residual stresses that is greater at the wavelength of 1064nm but at a lower depth.

In both cases the difference between one wavelength and another is most likely due to the greater hardness and depth of residual stresses present at the wavelength of 532nm.

Figure 5 shows the experimentally determined values for the coefficient of friction of Ti6Al4V. The friction coefficient was lower for the treated samples for both power densities: the values were 0.16 for a density of 7.5 GW/cm^2 and 0.18 for a density of 8.4 GW/cm^2, and that for the untreated specimen was 0.26.

3.2.2 Wear

Figure 6 shows the wear in the untreated specimen. Grooves can be observed that are parallel to the direction of the sliding track. Figures 7(a) and 7(b) show the wear patterns, which were identified from the sliding tracks, in the LSP-treated samples for wavelengths of 532 nm and 1064 nm, respectively. Figure 7(a) shows that the wear particles had a flat morphology (plate or foil type), which is a characteristic of both dry and lubricated wear. This result is due to the discontinuous application of the normal force by the pin to the disk surface, which can cause fatigue on the surface. Furthermore, a separation of the metal particles can be observed, which can occur in regions subjected to friction or

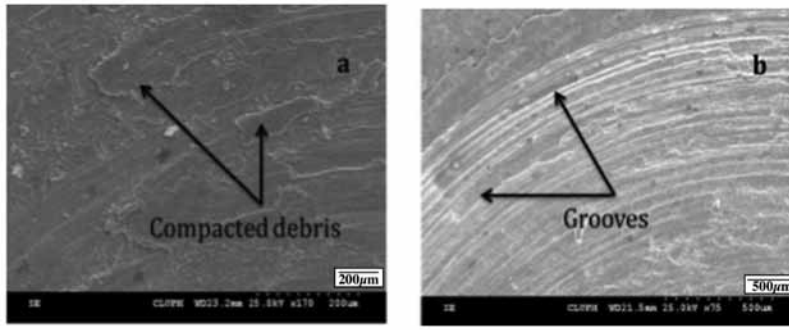

FIGURE 7
Wear systems after pin on disk test in LSP material treatment, a) at 532nm, b) at 1064nm.

relative motion, including cases where the material is soft [36]. Figure 7(b) shows that the surface of the specimen treated with a wavelength of 1064 nm has grooves in the abraded area that are of greater length and uniformity than those in the untreated specimen. These wear patterns were observed in the pin-on-disk test and were found in the material treated with LSP. This observation confirms that materials with an HCP crystal structure exhibit less adhesion than materials with a BCC or FCC crystalline structure [37, 38]. These results are consistent with those obtained in previous studies [24].

3.3 Metallographic analysis

Figure 8 no reduction in the grain size was observed at the surfaces of the treated specimens. The two characteristic phases, α and β, of the material remained unchanged.

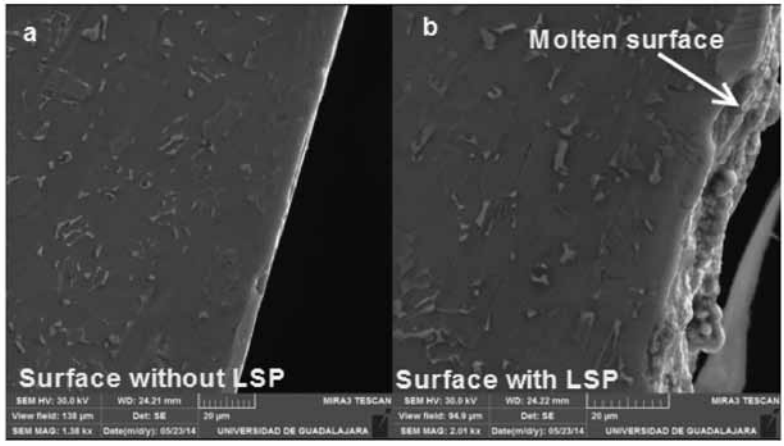

FIGURE 8
Surface microstructure of Ti6Al4V. A) without LSP. B) with LSP.

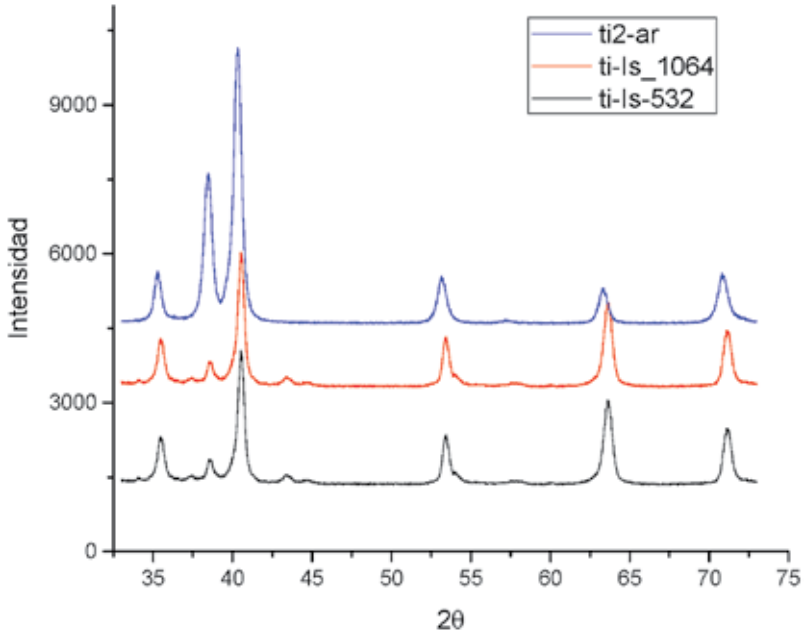

FIGURE 9
X-Ray diffraction pattern of laser peened samples red and black pattern, and blue pattern of untreated material.

3.4 Phase characterisation

The X-Ray diffraction tests did not show any phase changes or the formation of a different phase following LSP. Figure 9 shows the Miller indices of the crystallographic planes corresponding to the peaks in the X-Ray beam intensity as a function of the diffraction angle 2θ. The values for the 004 peak were shifted to the right with respect to the values for the untreated material. This result indicates the presence of residual compressive stresses in the material after being treated with LSP.

3.5 Micro-hardness tests

The hardness profiles by micro-indentation of the specimens are shown in Figure 10. The hardness in the first 250 μm was greater in the treated specimens than in the untreated specimen. The values of the micro-hardness of the untreated specimen were 303 and 294 (HV) at depths of 85 μm and 225 μm, respectively. In the sample treated with LSP at 7.5 GW/cm^2, the hardness values were 341 and 315 HV at the same two depths; i.e., the microhardness increased by 38 and 21 HV compared with the untreated specimen. In the specimen treated with LSP at 8.4 GW/cm^2, the hardness values obtained were 326 and 303 HV at the same two depths. Therefore, increases of 23 HV and 9 HV over those of the untreated specimen were obtained. The standard error

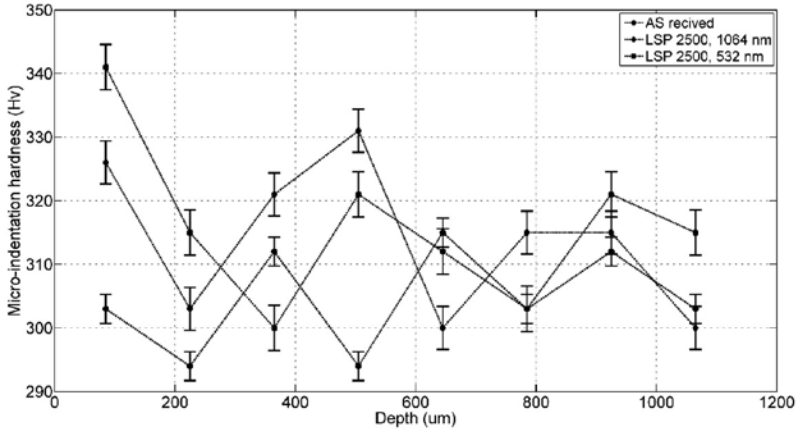

FIGURE 10
Measurement of micro-indentation harness profile on the specimen cross section. Samples treated with 532 nm and 1064 nm wavelengths.

calculated of hardness test was at range from to 2 and 4 HV. Tests of the hardness of the surface of Ti6Al4V treated with LSP have been previously reported [39].

3.6 Surface roughness

Figure 8 (b) shows the melt surface of Ti6Al4V alloy, rapid heating and fusing and the high pressure of the plasma generated by the laser pulse cause the liquefied material to be ejected from the centre to the periphery of the laser spot. This effect is shown in Figure 11. The ejected material is rapidly cooled by the water layer covering the surface of the material, resulting in an increase in surface roughness. The surface roughness is further increased by the overlapping of the laser pulses. The surface roughness values (Ra, arithmetic profile deviation) of the samples are shown in Table 3 for the two power densities. Despite the increase in the final surface roughness of the samples treated with LSP, no further surface finishing is required because the surface uniformity is greater than that obtained by abrasive blasting [24].

4 DISCUSSION

Because the water film confines the plasma generated by LSP, the surface temperature reaches approximately 2200 °C (the melting temperature of Ti64 is between 1604 and 1660 °C) [40]. This high temperature vaporises and melts the surface material, which rapidly cools, causing hardening. The interaction of the plasma with an aqueous environment generates an oxide film of approximately 1 μm in thickness, which is deposited on the surface and dif-

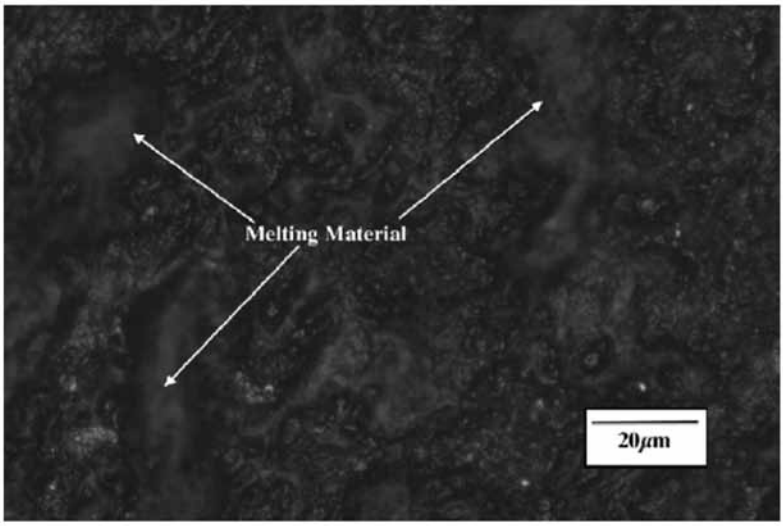

FIGURE 11
Unfocused areas show molten material after LSP treatment.

TABLE 3
Ra superficial roughness values.

Equipment	Base Material (Ra)	1064 nm	532 nm
Laser confocal Microscope	0.7454 μm0.5	2.9261 μm0.5	2.8821 μm

fuses into the material [14]. This combination of oxidation and surface hardening could affect the tribological properties of Ti6Al4V.

In the coupling phase of the tribological pair, variations in the friction force occur because the interaction between the two materials is slightly unstable causing skipping to occur (loading and unloading of the normal force). At this stage, the coefficient of friction is not stable because of differences in the roughness and the hardness of the two materials that constitute the tribological pair.

In the second stage, when the tribological pair stabilises, the oxide layer deposited on the surface acts as a lubricant. At this stage, because of the aforementioned properties and the increase in hardness, the friction coefficient decreases from 0.26 for the untreated specimen to 0.16 for the specimen treated with a power density of 7.5 GW/cm^2 and to 0.18 for the specimen treated with a power density of 8.4 GWm^2. The surface roughness due to the expulsion of molten material during the treatment increases considerably, from 0.7454 μm for the untreated specimen to 2.8821 μm for the specimen treated with a 7.5 GW/cm^2 power density and to 2.9261 μm for the specimen treated with an 8.4 GW/cm^2 power density. This change in roughness does

not have a significant effect regardless of the friction load applied in the test, as reported in the literature [41]. The change in the surface hardness induced by LSP is consistent to a depth of approximately 250 μm. The friction coefficient remains constant with the surface roughness.

In the third stage, greater wear was observed in the treated surface at depths greater than 250 μm. This difference is the result of material emission during the test. Figure 4(a) shows the transitions in which the pin penetrates the Ti6Al4V and the subsequent re-stabilization of the tribological pair for short periods as the effect of the induced hardness for the treatment with a 7.5 GW/cm^2 power density begins to decrease. In Figure 4(b), it can be observed that the transitions are much smoother and that stabilisation of the tribological pair occurs a second time because the effect of the induced hardness for the treatment with an 8.4 GW/cm^2 power density persists.

5 CONCLUSIONS

The surface residual compressive stresses in specimens of Ti6Al4V treated with Laser shock processing (LSP) increased by 257.14% in specimens treated at a power density of 8.4 GW/cm^2 and a wavelength of 1064 nm; and by 93% in specimens treated with a power density of 7.5 GW/cm^2 at 532 nm compared with the untreated specimen. The power density has an important role in the magnitude and depth of the residual compressive stresses.

The friction force was stable over a greater duration in the specimens treated with LSP. The friction coefficient decreased by 38.5% and 30.5% for specimens treated with a power density of 7.5 GW/cm^2 and 8.4 GW/cm^2, respectively. These results represent an increase in the period of stability of the frictional force of 475.19% and 350% for the specimens treated at a power density of 7.5 GW/cm^2 and 8.4 GW/cm^2, respectively, compared with the untreated specimen.

No phase changes were observed in the alloy following LSP. The crystallographic peaks decreased slightly in intensity, and the widths increased. It is possible that these changes were due to LSP.

The surface hardness at a depth of 225 μm increased by 19% in specimens treated with a 7.5 GW/cm^{2}power density and by 10% in specimens treated with an 8.4 GW/cm^2 power density compared with the untreated specimen. This increase may have been caused by the presence of oxides on the irradiated surface. The decrease in the friction coefficient corresponded to an increase in the surface hardness of the specimens treated with LSP.

The surface roughness of the specimens increased by 392.5% for the specimens treated with LSP at an 8.4 GW/cm^2 power density and by 386.6% for the specimens treated with LSP at a 7.5 GW/cm^2 power density compared to that of the untreated specimen. Despite this increase, the surface quality remained satisfactory and would be acceptable for biomedical applications.

The wear in the treated and untreated specimens exhibited damage at the periphery of the pin test disk. In future research, depths from 0 to 250 μm, where changes due to LSP have been observed, they will be analysed in a later article.

In this study, LSP was tested on Ti6Al4V specimens without an ablative protection layer and using two different wavelengths. LSP can be used with two forms of confinement, waterjet and total immersion. These options are satisfactory in improving the mechanical properties, including residual stresses, the coefficient of friction, the surface hardness and the surface roughness.

6 ACKNOWLEDGEMENTS

The authors would like to thank the Centre for Engineering and Industrial Development (CIDESI) of Queretaro; the U.P.M. Laser Centre, Madrid, Spain; the Departments of Physics and Project Engineering at the University of Guadalajara for providing the facilities used in this research; and the National Council of Science and Technology (CONACYT) for the award of a postgraduate scholarship.

REFERENCES

[1] Altenberger, I., Nalla, R.K., Sano, Y., Wagner, L., Ritchie, R.O. On the effect of deep-rolling and laser-peening on the stress-controlled low- and high-cycle fatigue behaviour of Ti–6Al–4V at elevated temperatures up to. *Int. J. Fatigue,* **44** (2012), 292-302.

[2] ASTM. *E-837-01, Standard Test Method for Determining Residual Stresses by the Hole Drilling Strain Gage Method,* (2002), ASTM International, (v.03.01).

[3] ASTM, G. (2004), 99-04 Standard test method for Wear testing with a pin on disk apparatus ASTM International.

[4] ASTM. (2012), E-3-11, Standard Guide for preparations of metallographic specimens, ASTM International, (v.03.01).

[5] ASTM. (2011), E384 11-1 Standard test method for Knoop and Vickers hardness of materials, ASTM International, (v.03.01).

[6] Bagherifard, S., Ghelichi, R., Guagliano, M. Numerical and experimental analysis of surface roughness generated by shot peening. *Appl. Surf. Sci.,* **258** (2012), 6831-6840. doi: 10.1016/j.apsusc.2012.03.111.

[7] Buckley, D.H. *Surface Effects in Adhesion, Friction, Wear, and Lubrication, Tribology Series* (1981), Amsterdam: Elsevier.

[8] Campbell F.C. Titanium. In Campbell, F.C. (ed.), Chapter 28, *Elements of Metallurgy and Engineering Alloys*. Materials Park, OH: ASM International, 2008, pp 527-545.

[9] Castañeda, E., Rubio-Gonzalez, C., Chavez-Chavez, A., Gomez-Rosas, G. Laser shock processing with different conditions of treatment on duplex stainless steel. *J. Mater. Eng. Perform.*, **24** (2015), 2521-2525.

[10] Clauer, A.H., Holbrook, J.H. Effects of laser induced shock waves, rate phenomena in metals. In: Meyers, M.A. et al. (ed.), Chapter 38, *Shock Waves and High-Strain-Rate Phenomena in Metals*. New York, NY: Plenum Press. 1981. pp 675-703.

[11] Fairand, B.P., Clauer, A.H., Jung, R.G., Wilcox, B.A. Quantitative assessment of laser-induced stress waves generated at confined surfaces. *Appl. Phys. Lett.,* **25** (1974), 431-433. doi: 10.1063/1.1655536.

[12] Gil, F.J., Crespo, A., Manero, J.M., Rodriguez, D., Planell, J.A. Mejora de la resistencia al desgaste de titanio y sus aleaciones utlizados para prótesis articulares. *Biomecanica.,* **10** (2002), 20-37.

[13] Gomez-Rosas, G., Rubio-Gonzalez, C., Ocaña, J.L., Molpeceres, C., Porro, J.A., Morales, M., Casillas, F.J. Laser shock processing of 6061-T6 Al alloy with 1064 nm and 532 nm wavelengths. *Appl. Surf. Sci.,* **256** (2010), 5828-5831. doi: 10.1016/j.apsusc.2010.03.043.

[14] Gomez-Rosas, G., Rubio-Gonzalez, C., Ocaña, J.L., Molpeceres, C., Porro, J.A., Chi-Moreno, W., Morales, M. High level compressive residual stresses produced in aluminum alloys by laser shock processing. *Appl. Surf. Sci.,* **252** (2005), 883-887. doi: 10.1016/j.apsusc.2005.01.150.

[15] Golden, P.J., Hutson, A., Sundaram, V., Arps, J.H. Effect of surface treatments on fretting fatigue of Ti–6Al–4V. *Int. J. Fatigue,* **29** (2007), 1302-1310. doi: 10.1016/j.ijfatigue.2006.10.005.

[16] Hu, Y., Yao, Z. Overlapping rate effect on laser shock processing of 1045 steel by small spots with Nd:YAG pulsed laser. *Surf. Coat. Technol.,* **202** (2008), 1517-1525. doi: 10.1016/j.surfcoat.2007.07.008.

[17] Khosroshahi, M.E., Mahmoodi, M., Tavakoli, J. Characterisation of Ti6Al4V implant surface treated by Nd:YAG laser and emery paper for orthopaedic applications. *Appl. Surf. Sci.,* **253** (2007), 8772-8781. doi: 10.1016/j.apsusc.2007.04.084.

[18] Kumar, D., Nadeem Akhtar, S., Kumar Patel, A., Ramkumar, J., Balani, K. Tribological performance of laser peened Ti–6Al–4V. *Wear,* **322** (2015), 203-217. doi: 10.1016/j.wear.2014.11.016.

[19] Liu, H.X., Hu, Y., Wang, X., Shen, Z.B., Li, P., Gu, C.X., Liu, H., Du, D.Z., Guo, C. Grain refinement progress of pure titanium during laser shock forming (LSF) and mechanical property characterisations with nanoindentation. *Mater. Sci. Eng. A,* **564** (2013), 13-21. doi: 10.1016/j.msea.2012.11.087.

[20] Luengo, L., Oliver: Final Project, School of Industrial Engineering of Barcelona, Es. 2008.

[21] Menezes, P.L., Kishore, K., Kailas, S.V. Influence of roughness parameters on coefficient of friction under lubricated conditions. *Sadhana,* **33** (2008), 181-190. doi: 10.1007/s12046-008-0011-8.

[22] Morales, M., Ocaña, J.L., Molpeceres, C., Porro, J.A., García-Beltrán, A. Model based optimization criteria for the generation of deep compressive residual stress fields in high elastic limit metallic alloys by ns-laser shock processing. *Surf. Coat. Technol.,* **202** (2008), 2257-2262. doi: 10.1016/j.surfcoat.2007.12.007.

[23] Peyre, P., Carboni, C., Forget, P., Beranger, G., Lemaitre, C., Stuart, D. Influence of thermal and mechanical surface modifications induced by laser shock processing on the initiation of corrosion pits in 316L stainless steel. *J. Mater Sci*, **42** (2007), 6866-6877. doi: 10.1007/s10853-007-1502-4.

[24] Peyre, P., Fabbro, R., Berthe, L., Dubouchet, C. Laser shock processing of materials, physical processes involved and examples of applications. *J. Laser Appl.,* **8** (1996), 135-141. doi: 10.2351/1.4745414.

[25] Porro, J.A., Molpeceres, C., Morales, M., Ocaña, J.L. Generación de un campo de tensiones residuales de compresión en aluminio 2024-t351 mediante tratamiento por onda de choque generada por láser (laser shock processing). Óptica Pura y Aplicada, **40** (2007), 73-78.

[26] Rozmus, M., Kusiński, J., Blicharski, M., Marczak, J. Laser shock peening of a Ti6Al4V titanium alloy. *Arch. Metall. Mater.*, **54** (2009), 665-670.

[27] Rozmus-Górnikowska, M. Surface modifications of a Ti6Al4V alloy by a laser shock processing. *Acta Phys. Pol. A*, **117** (2010), 808-811.

[28] Rubio-González, C., Felix-Martinez, C., Gomez-Rosas, G., Ocaña, J.L., Morales, M., Porro, J.A. Effect of laser shock processing on fatigue crack growth of duplex stainless steel. *Mater. Sci. Eng. A,* **528** (2011), 914-919. doi: 10.1016/j.msea.2010.10.020.

[29] Sano,Y., Obata, M., Kubo, T., Mukai, N., Yoda, M., Masaki, K., Ochi, Y. Retardation of crack initiation and growth in austenitic stainless steels by laser peening without protective coating. *Mater. Sci. Eng. A*, **417** (2006), 334-340. doi: 10.1016/j.msea.2005.11.017.

[30] Sano, Y., Mukai, N., Okazaki, K., Obata, M. Residual stress improvement in metal surface by underwater laser irradiation. *Nucl. Instrum. Methods Phys. Res. Sect. B,* **121** (1997), 432-436. doi: 10.1016/S0168-583X(96)00551-4.

[31] Sano, Y., Akita, K., Masaki, K., Ochi, Y., Altenberger, I., Scholtes, B. Laser peening without coating as a surface enhancement technology. *Journal of Laser Micro Nanoengineering,* **1** (2006), 161-166.

[32] Sánchez-Santana, U., Rubio-González, C., Gomez-Rosas, G., Ocaña, J.L., Molpeceres, C., Porro, J., Morales, M. Wear and friction of 6061-T6 aluminum alloy treated by laser shock processing. *Wear,* **260** (2006), 847-854. doi: 10.1016/j.wear.2005.04.014.

[33] Sirosky, M.E. Transactions ASME, series D. *Journal of Basic Engineering,* **85** (1963), 279-285.

[34] Sokol, D., Laser shock processing. Technical Bulletin 1, Dublin, OH: Laser Technologies Inc.

[35] Trtica, M., Gakovic, B., Batani, D., Desai, T., Panjan, P., Radak, B. Surface modifications of a titanium implant by a picosecond Nd:YAG laser operating at 1064 and 532 nm. *Appl. Surf. Sci.,* **253** (2006), 2551-2556. doi: 10.1016/j.apsusc.2006.05.024.

[36] Trdan, U., Grum, J. Evaluation of corrosion resistance of AA6082-T651 aluminium alloy after laser shock peening by means of cyclic polarisation and ElS methods. *Corros. Sci.* **59** (2012), 324-333. doi: 10.1016/j.corsci.2012.03.019.

[37] Trdan U, Porro JA, Ocaña JL, Grum J. Laser shock peening without absorbent coating (LSPwC) effect on 3D surface topography and mechanical properties of 6082-T651 Al alloy. *Surf. Coat. Technol.,* **208** (2012), 109-116.

[38] Yakimets, I., Richard, C., Béranger, G., Peyre, P. Laser peening processing effect on mechanical and tribological properties of rolling steel 100Cr6. *Wear,* **256** (2004), 311-320. doi: 10.1016/S0043-1648(03)00405-8.

[39] Yue, L., Wang, Z., Li, L. Material morphological characteristics in laser ablation of alpha case from titanium alloy. *Appl. Surf. Sci.,* **258** (2012), 8065-8071. doi: 10.1016/j.apsusc.2012.04.173.

[40] Zhang, X.C., Zhang, Y.K., Lu, J.Z., Xuan, F.D., Wang, Z.D., Tu, S.T. Improvement of fatigue life of Ti–6Al–4V alloy by laser shock peening. *Mater. Sci. Eng. A,* **527** (2010), 3411-3415.

[41] Ziwen, C., Shuili, G., Shikun, Z., Zhigang, C. Surface profiles and residual stresses on Laser shocked Zone of Ti6Al4V titanium alloy. *Rare Metal Mat. Eng.*, **40** (2011), 190-193.